

Dehydration of D-xylose over SiO₂-Al₂O₃ catalyst: Perspective on the pathways for condensed products

Su Jin You*, Eun Duck Park^{*,**}, and Myung-June Park^{*,**,*†}

*Department of Energy Systems Research, Ajou University, Suwon 16499, Korea

**Department of Chemical Engineering, Ajou University, Suwon 16499, Korea

(Received 9 June 2015 • accepted 11 November 2015)

Abstract—This work addresses the kinetic mechanism for the dehydration of D-xylose over the SiO₂-Al₂O₃ solid catalyst, where the formation of condensed products is included in addition to the production of furfural and its decomposition. The kinetic modeling and parametric sensitivity show that the isomerization of D-xylose takes place in the early stages of the reaction, followed by the dehydration of isomers. Accordingly, the homogeneous polymerization of isomers is found to be dominant. The developed model is used to evaluate the effects of operating conditions on the catalytic performance; high temperature and D-xylose concentration guarantee high furfural yield.

Keywords: D-Xylose, Furfural, Dehydration, Silica-alumina, Kinetic Modeling

INTRODUCTION

The increasing CO₂ concentration in the atmosphere and limited reserves of fossil fuels have motivated the development of green processes with sustainable and environmentally friendly feed stocks in place of fossil fuels. Lignocellulosic biomass, which is a potential renewable feed stock for replacing fossil fuels in the chemical industry, is typically composed of cellulose, hemicellulose, and lignin, which can be transformed into a variety of chemicals through biological and chemical processes. Furfural, which can be made from hemicellulose, is an important intermediate in a broad range of applications such as nylon, lubricants, solvents, adhesives, medicine, and plastics. Furfural has also been reported to be upgraded to furanic biofuels via hydrogenation, rearrangement, and C-C coupling [1].

Furfural can be produced through the dehydration of pentoses, which are abundant in agricultural raw materials including corn-cobs, oat hulls, bagasse, cottonseed hull bran, cottonseed hulls, and rice hulls [2]. The commercial process for furfural, that is, the Quaker Oats process, uses sulfuric acid as a homogeneous catalyst and a significant amount of steam. Therefore, this process suffers from corrosion and safety problems and involves considerable cost for the separation of sulfuric acid from the products and its neutralization [2]. Since other processes based on homogeneous catalysts (supercritical water [3], hydrochloric acid [4,5], sulfuric acid [6,7], formic acid [8]) also have the same drawbacks, much attention has been paid to the dehydration of D-xylose to furfural over heterogeneous catalysts, such as microporous zeolites and related materials [9,10], modified mesoporous silica [11-14], Amberlyst [15], Keggin-type heteropolyacids [16], titanates and niobates [17], hydroxylated MgF₂ [18], and metal oxides (TiO₂, ZrO₂, Zr-WO₆, VPO_x, SnO₂, SiO₂-Al₂O₃) [19-23]. Among these solid acid catalysts, SiO₂-

Al₂O₃ has been reported to be stable, commercially available, and used in various reactions including fluid catalytic cracking, hydrocracking, and hydrogenation [24]. Furthermore, the controllable surface acidity and the presence of mesopores are advantages of SiO₂-Al₂O₃ catalysts for this reaction.

A number of byproducts are formed during this reaction. In particular, humin formation is critical in suppressing the catalyst stability. However, most previous reports have focused on the kinetics of the main reaction (from D-xylose to furfural), with the decomposition considered to be only a side reaction. Thus, there has been little effort devoted to investigating the mechanism for the production of soluble polymers (condensed products), although a detailed kinetic study for each product is quite important for an understanding of the reaction pathway and determination of the optimum reaction conditions. In addition, despite many reported kinetic models for homogeneous [3,5,6,8,25] and heterogeneous [26,27] catalytic systems, no detailed kinetic study has been reported on the dehydration of D-xylose over the SiO₂-Al₂O₃ catalyst. In the present study, a detailed kinetic model is developed for this reaction to understand the reaction pathways for the formation of both furfural and condensed products, and to evaluate the effects of the operating conditions on the catalytic performance of the SiO₂-Al₂O₃ catalyst.

EXPERIMENTAL

The solid acid catalyst, SiO₂-Al₂O₃, was purchased from a commercial vendor (ZEOCHEM, ZEObeadsTM WS) and calcined in air at 600 °C before the reaction. The alumina content was 3.55 wt% [28]. The BET surface area and micropore surface area were 559 m²/g and 82 m²/g, respectively [28]. The total acid sites amounted to 207 μmol NH₃/g, and the ratio of the number of Brønsted acid sites to total acid sites was 0.44 [28].

The catalytic activity was measured under isothermal conditions with operating conditions varied between 160 and 200 °C, while a preheater was installed to heat the feed to 80 °C. The reaction pressure

[†]To whom correspondence should be addressed.

E-mail: mjpark@ajou.ac.kr

Copyright by The Korean Institute of Chemical Engineers.

Table 1. Experimental conditions and measured data used in the parameter estimation

No.	Conditions			D-Xylose conversion [%]	Measured data		
	Space velocity [m ³ /(g _{cat} ·h)]	Temperature [°C]	D-Xylose concentration [wt%]		Selectivity [%]		
					Furfural	Isomer	Condensed products
1	11×10 ⁻⁶	160	1	33.1	18.9	52.8	10.9
2			3	33.5	16.0	51.9	17.6
3			5	45.6	21.6	39.4	20.8
4		180	1	65.0	33.6	31.7	7.8
5			3	68.8	28.6	28.0	19.8
6			5	76.4	26.1	22.9	29.4
7		200	1	89.2	32.9	13.7	23.8
8			3	93.2	24.8	8.3	43.9
9			5	90.0	24.0	14.1	41.0
10	44×10 ⁻⁶	160	1	18.8	6.2	69.2	13.3
11			3	22.1	8.5	71.2	7.6
12			5	22.6	8.1	55.5	26.5
13		180	1	28.1	10.2	65.3	11.1
14			3	32.5	11.0	61.1	13.4
15			5	43.5	12.2	47.8	26.7
16	200	1	51.2	16.9	46.9	16.7	
17		3	58.9	20.3	36.7	23.3	
18		5	56.4	16.4	37.2	29.1	

was maintained at 3.0 MPa by a backpressure regulator (TESCOM). Products were collected in a cold trap maintained at room temperature and sampled every 4 h for analysis (for the 12 h duration of the experiment). Detailed experimental conditions are listed in Table 1. Note that the solid acid catalyst can be deactivated due to some causes, one of which is carbon deposition, occurring in the initial stage of the reaction. Since the catalytic activity decreased slowly during the course of the reaction for a long time, it was assumed that deactivation did not mislead us about the activity data in this work.

Liquid products were filtered with a 0.2- μ m membrane filter and analyzed using an HPLC instrument (Waters 1525 Binary HPLC pumps, YL 9110 quaternary pump) equipped with a 2487 dual-wavelength absorbance detector (Waters) at 210 nm for furfural, and refractometer detector (Water, YL 9170 RI detector) for D-xylose, lyxose, xylulose, aldehydes, dihydroxyacetone, and organic acids. To separate the D-xylose, lyxose, and xylulose in the aqueous-phase, a Ca²⁺-form ion exchange column (PL Hi-Plex Ca 300×7.7, Agilent) was used. Products such as aldehydes, dihydroxyacetone, and organic acids were separated using the Ca²⁺-form ion exchange column (PL Hi-Plex Ca 300×7.7, Agilent) and a H⁺-form ion exchange column (Aminex HPX-87H, BIORAD) with 0.01 M H₂SO₄ solution. The D-xylose conversion ($X_{D\text{-xylose}}$), the molar carbon yield (Y_i), and the molar carbon selectivity (S_i) were calculated using the following equations:

$$X_{D\text{-xylose}} [\%] = (N_{D\text{-xylose},0} - N_{D\text{-xylose}}) / N_{D\text{-xylose},0} \times 100 \quad (1)$$

$$Y_i [\%] = N_i / N_{D\text{-xylose},0} \times 100 \quad (2)$$

$$S_i [\%] = N_i / (N_{D\text{-xylose},0} - N_{D\text{-xylose}}) \times 100 \quad (3)$$

where $N_{D\text{-xylose},0}$ and $N_{D\text{-xylose}}$ represent the moles of carbon in D-xylose at the inlet and the outlet of the reactor, respectively, while N_i is the moles of carbon of species (i) in the product. Because humin could not be detected by HPLC, the yield of humin (Y_{humin}) was calculated by subtracting the sum of the other products' yields from D-xylose conversion.

RESULTS AND DISCUSSION

A reaction pathway for the dehydration of xylose over solid acid catalysts, suggested in the present study, is shown in Fig. 1. Since the dehydration of xylulose (one of the isomers of D-xylose) into furfural is faster than the direct conversion of D-xylose into furfural (activation energies for the dehydration of D-xylose and xylulose are 134 and 97 kJ/mol, respectively [29]), two consecutive steps were considered in the present study: the isomerization of D-xylose to xylulose or lyxose (step 1), and their subsequent dehydration to furfural (step 2) [30]. Note that L-xylose, isomer of D-xylose, was not considered in the present study due to difficulties in detection. The isomerization of D-xylose is reported to occur either by the rearrangement of a functional group or through a change in configuration around the C1 and C2 carbon atoms [30]. Some researchers have suggested the reversible isomerization of D-xylose [3], while others assumed an irreversible process [8,31]. In the present study, irreversible isomerization was assumed since it was difficult to calculate the Gibbs energy for the equilibrium constant owing to the existence of many kinds of isomers.

The decomposition of D-xylose (step 3) has been identified from the retro-aldol condensation reactions of D-xylose in water at high

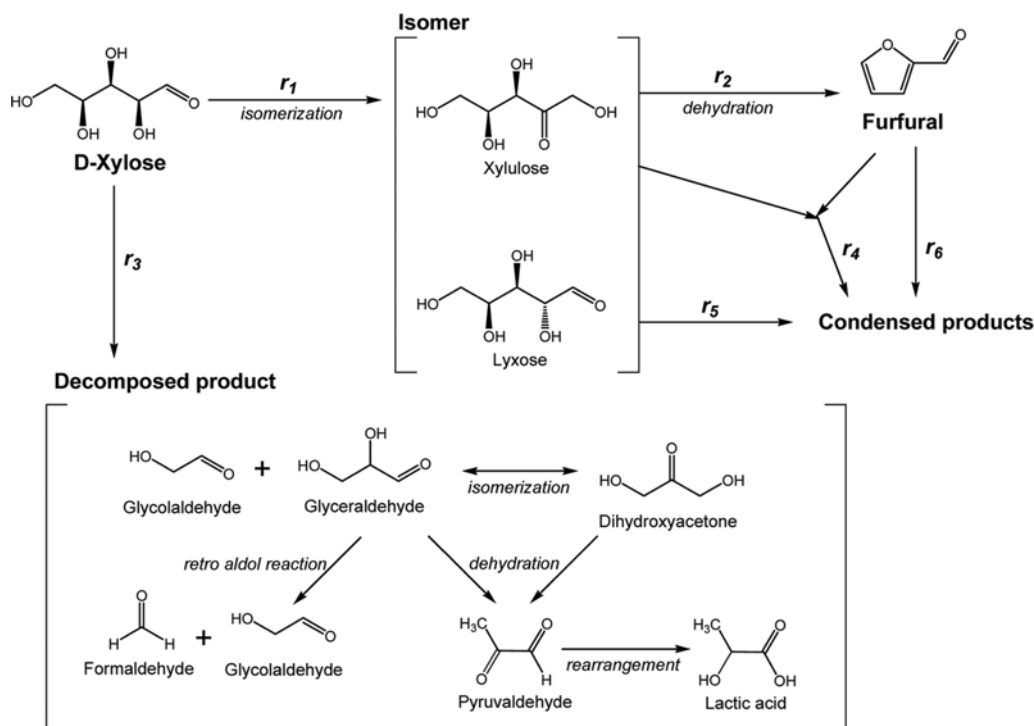


Fig. 1. Reaction pathway for the dehydration of D-xylose to furfural.

temperature [3]. The species obtained from the decomposition of D-xylose include glycolaldehyde, dihydroxyacetone, and glyceraldehyde; glyceraldehyde can be further converted to formaldehyde through the retro-aldol condensation reaction [3]. In addition, the dehydration of either glyceraldehyde or dihydroxyacetone produces pyruvaldehyde, which is further converted to lactic acid through rearrangement [3]. Although acetaldehyde was detected by HPLC analysis in the present study, no convincing hypothesis for its formation by the decomposition of D-xylose has yet been reported. Formic acid has been reported to be produced from the rehydration of D-xylose and/or a fragment of furfural [27,32]. However, trace amounts of formic acid and other organic acids [3,8,27,33] were observed here. Therefore, the oxidation of furfural to organic acids such as 2-furoic acid, which may reduce the yield of furfural, was not considered. Notably, some researchers have reported that furfural can also be decomposed. However, our previous experiments [23], in which furfural was fed to the catalytic reactor, showed no existence of decomposed products, and thus, the decomposition of furfural was neglected in the present study.

In addition to D-xylose, isomers, furfural, and decomposed products (directly measurable by HPLC analysis [28]), it was found from the carbon balance that unmeasurable products existed, which were assumed to be condensed from isomers and furfural. The corresponding pathways were taken into account (steps 4-6); Dee and Bell [34] suggested that humin (one of the condensed products) can be produced via the condensation polymerization of furan and glucose. As an analogy, the heterogeneous polymerization of furfural and isomers was suggested in the present study (step 4). Additionally, Ferreira et al. [26] identified humin as one of the soluble polymers, consisting of aliphatic and aromatic compounds includ-

ing furan and/or benzene rings. Recently, van Putten et al. [35] discussed humin formation, and there are several reported works on the condensation of furfural via Diels-Alder reaction [36,37]. Despite the plausible heterogeneous condensation reported in the literature, there is also a possibility of homogeneous condensation for the formation of condensed products. Therefore, two additional steps (condensations of isomers and furfural, in steps 5 and 6, respectively) were included in the reaction mechanism.

For the development of the reaction rates, a power-law model was assumed for each reaction step. A heterogeneous model was not considered because information on the existence of intermediate species on the surface was available neither in the literature nor in our experimental data. In addition, one of the purposes of the present study was the comparison between three possible reactions for the formation of condensed products, and thus, it was assumed that a simple reaction rate would be enough. Kinetic parameters and reaction orders were estimated using the "lsqcurvefit" subroutine in MATLAB (MathWorks, Inc.), in which the Levenberg-Marquardt method is applied. Since the number of elements in the objective function which should be minimized in the estimation was 4 (conversion and 3 selectivities; cf. Table 1), the total number of independent data used in the minimization was 72. The number of data is approximately three-times more than that of parameters to be estimated. The resulting rates are as follows:

$$r_1 = 2.88 \times 10^{-4} \exp\left[\frac{-61,900}{R}\left(\frac{1}{T} - \frac{1}{T_{ref}}\right)\right] C_{xylose}^{1.29} \quad (4)$$

$$r_2 = 1.94 \times 10^{-3} \exp\left[\frac{-37,400}{R}\left(\frac{1}{T} - \frac{1}{T_{ref}}\right)\right] C_{isomer}^{1.03} \quad (5)$$

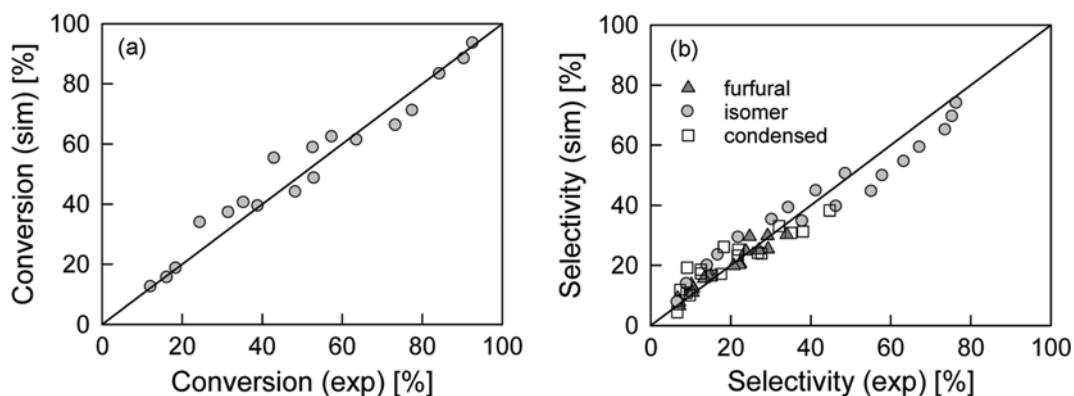


Fig. 2. Comparison of (a) xylose conversion and (b) selectivities between simulated results and experimental data.

$$r_3 = 5.07 \times 10^{-5} \exp\left[-\frac{82,300}{R}\left(\frac{1}{T} - \frac{1}{T_{ref}}\right)\right] C_{xylose}^{1.25} \quad (6)$$

$$r_4 = 2.05 \times 10^{-4} \exp\left[-\frac{50,200}{R}\left(\frac{1}{T} - \frac{1}{T_{ref}}\right)\right] C_{furfural}^{0.55} C_{isomer}^{0.19} \quad (7)$$

$$r_5 = 3.43 \times 10^{-6} \exp\left[-\frac{52,500}{R}\left(\frac{1}{T} - \frac{1}{T_{ref}}\right)\right] C_{isomer}^{2.46} \quad (8)$$

$$r_6 = 1.45 \times 10^{-9} \exp\left[-\frac{43,600}{R}\left(\frac{1}{T} - \frac{1}{T_{ref}}\right)\right] C_{furfural}^{1.14} \quad (9)$$

Here, the reaction rates (r) and concentrations (C) are in mol/(m³·s) and mol/m³, respectively, and the gas constant (R) is 8.314 J/(mol·K). The reference temperature (T_{ref}) was specified as 165 °C. Fig. 2 shows the parity plot for D-xylose conversion, and the selectivities of furfural, isomers, and condensed products, and satisfactory agreement between the experimental data and simulated results with the estimated parameters is observed. The mean of absolute relative residuals (MARR) values was calculated to be 8.3, 12.2, 16.0, and 20.2% for the D-xylose conversion, and the selectivities of furfural, isomers, and condensed products, respectively. Considering that the standard deviation of the measurement for either two or three repeated experiments was $\approx 15.1\%$, the MARR values were determined to be reasonable.

The validity of the estimated kinetic parameters was proven by comparison with the reported values. As shown in Table 2, the acti-

vation energy for the isomerization of D-xylose (step 1) ranges between 40 and 100 kJ/mol, and the estimated value in the present study (61.9 kJ/mol) is within this range. Meanwhile, the activation energy for the dehydration of isomers was estimated to be lower than the reported values.

For the formation of condensed products, the activation energies for all three pathways (steps 4–6) were estimated to be similar, while the reaction orders of steps 4 and 6 were determined to be lower than expected, indicating that step 5 might have a higher contribution than the others. Given the characteristics of condensation reactions, both reaction orders of step 4 ($n_{furfural}$ and n_{isomer}) were expected to be one, while the order of over two seemed to be reasonable for step 6. For quantitative analysis of the contribution of each step, the normalized parametric sensitivity, defined as the ratio of the fractional change of output to the fractional change of parameter $[(\Delta y/y)/(\Delta p/p)]$ was calculated, and the results are shown in Fig. 3. As shown, the effects of k_4 and k_6 on the conversion and selectivities are negligible compared with that of k_5 , indicating that homogeneous condensation of isomers is more dominant than the condensation involving furfural (steps 4 and 6). This feature can be explained by the time evolutionary behavior of the reactions. As shown in Fig. 4, the selectivity of the isomers decreased with decreasing space velocity (SV) (increasing residence time) while the furfural selectivity increased, suggesting that the isomerization

Table 2. Reported values of kinetic parameters

Catalyst type	Catalyst	Activation energy [kJ/mol]		
		E ₁	E ₂	E ₃
Homo- geneous	Hot water ^a [38]		77	59-154
	Formic acid [8]	155	142	147
	Sulfuric acid ^a [39]		84	
	Hydrochloric acid ^a [40]		48	
	Hydrochloric acid ^a [5]		124	
	(HCl & SnCl ₂) [29]	65	97	
Hetero- geneous	(H-ZSM-5) [27]	40-97	98	

^aDirect dehydration of xylose into furfural was considered

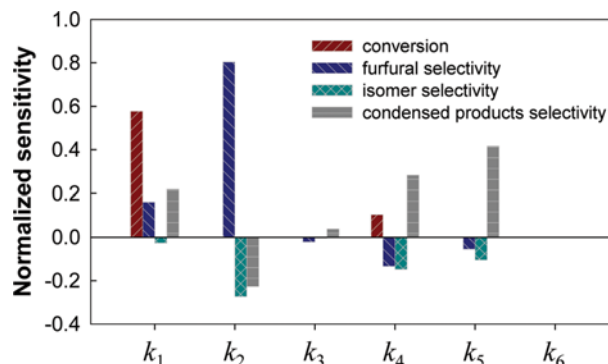


Fig. 3. Normalized parametric sensitivity on the xylose conversion, and the selectivities of furfural, isomers, and condensed products, when the temperature, xylose concentration, and SV were 180 °C, 3 wt%, and 30 mL/(g_{cat}·h), respectively.

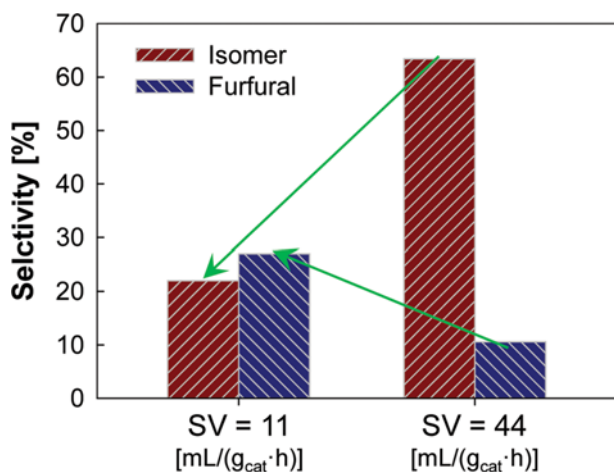


Fig. 4. Experimentally measured selectivities of isomers and furfural, when the temperature and xylose concentration were 180 °C and 3 wt%, respectively.

of D-xylose takes place in the early stages of the reaction, and then the produced isomers are dehydrated to furfural. Therefore, the condensation of isomers occurs prior to the other condensation reactions involving furfural. Although the products by r_3 (the condensation of isomers) are unidentifiable, on the basis of other reports, the major component of the condensed products by reactions r_4 and r_6 (furfural involved) might be humin [26,34].

The effects of D-xylose concentration and temperature were investigated by using the developed reaction rates (see Fig. 5). Positive effects of both concentration and temperature were shown for the conversion (Fig. 5(a)), while a slightly negative effect of concentration on the furfural selectivity was shown at high temperatures (Fig. 5(b)). However, the highest yield of furfural was obtained under conditions of high concentration and high temperature.

As discussed above, when the reaction proceeds further, more isomers are dehydrated to furfural, and thus, the isomer selectivity decreases with increasing conversion (Fig. 5(c)). On the other hand, the selectivity of condensed products also increases with decreasing isomer selectivity, probably owing to the trigger of r_3 and r_6 by the production of furfural.

CONCLUSIONS

A kinetic mechanism for the dehydration of D-xylose over the SiO₂-Al₂O₃ solid catalyst has been suggested on the basis of experimental observations and reported results. In addition to well-known pathways for the production of furfural and decomposed products, the suggested mechanism includes the formation of condensed products in both homogeneous and heterogeneous polymerizations. The developed kinetic model successfully describes the experimental results, and further analysis shows a time evolutionary reaction procedure: isomerization and the condensation of isomers, followed by their dehydration to furfural and condensation leading to the formation of (probably) humin. It is concluded that the

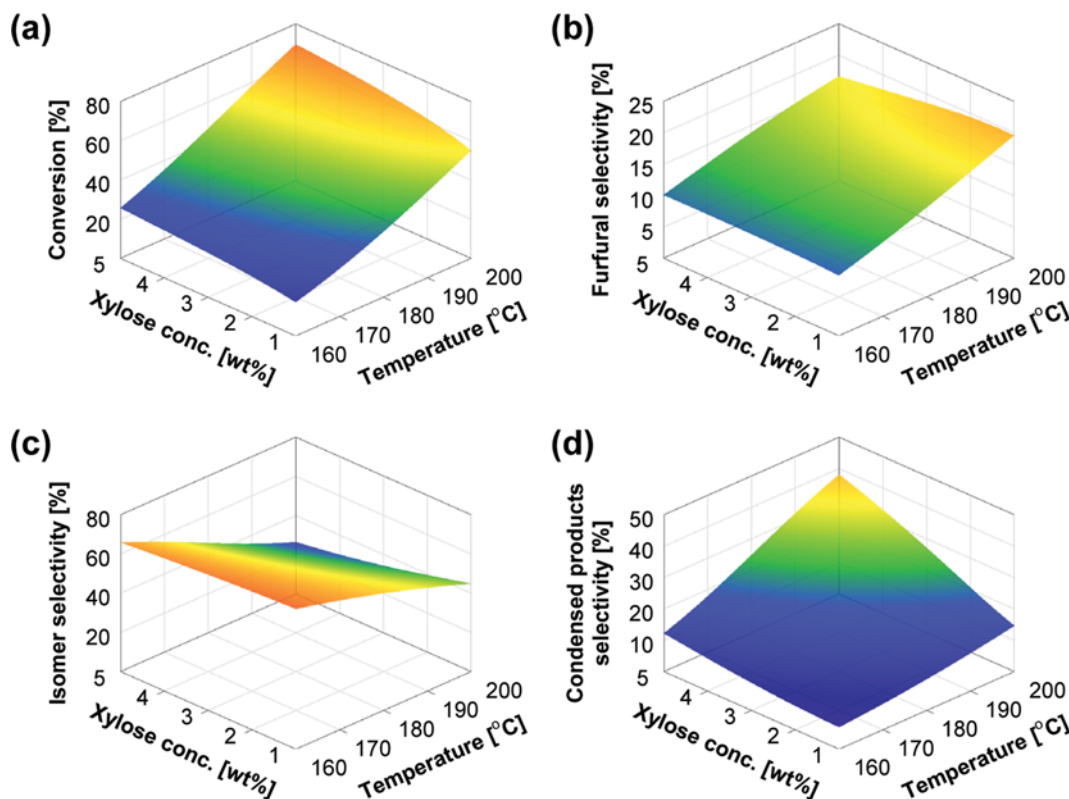


Fig. 5. Effects of xylose concentration and temperature on (a) xylose conversion, and the selectivities of (b) furfural, (c) isomers, and (d) condensed products, when the SV was 30 mL/(g_{cat}·h).

kinetic model in the present study can be used to better understand the governing reactions over the SiO₂-Al₂O₃ solid catalyst, and will be applied to provide useful information on the scale-up of the reactor and the optimal operating conditions.

ACKNOWLEDGEMENTS

This work was supported by the Priority Research Centers Program through the National Research Foundation of Korea (NRF) funded by the Ministry of Education, Science and Technology (2009-0094047). It was also supported financially by a grant from the Industrial Source Technology Development Programs (10032003) of the Ministry of Knowledge Economy (MKE) of Korea.

REFERENCES

- J.-P. Lange, E. van der Heide, J. van Buijtenen and R. Price, *ChemSusChem*, **5**, 150 (2012).
- K. J. Zeitsch, *The Chemistry and Technology of Furfural and its Many By-products*, Elsevier Science, Amsterdam (2000).
- T. M. Aida, N. Shiraishi, M. Kubo, M. Watanabe and R. L. Smith Jr., *J. Supercrit. Fluids*, **55**, 208 (2010).
- S. Wang, Y. Du, P. Zhang, X. Cheng and Y. Qu, *Korean J. Chem. Eng.*, **31**, 2286 (2014).
- R. Weingarten, J. Cho, J. W. C. Conner and G. W. Huber, *Green Chem.*, **12**, 1423 (2010).
- M. J. Antal Jr., T. Leesomboon, W. S. Mok and G. N. Richards, *Carbohydr. Res.*, **217**, 71 (1991).
- S. Kim, J. Lee, X. Yang, J. Lee and S. Kim, *Korean J. Chem. Eng.*, **32**, 2280 (2015).
- K. Lamminpää, J. Ahola and J. Tanskanen, *Ind. Eng. Chem. Res.*, **51**, 6297 (2012).
- C. García-Sancho, I. Sádaba, R. Moreno-Tost, J. Mérida-Robles, J. Santamaría-González, M. López-Granados and P. Maireles-Torres, *ChemSusChem*, **6**, 635 (2013).
- S. Lima, M. M. Antunes, A. Fernandes, M. Pillinger, M. F. Ribeiro and A. A. Valente, *Appl. Catal. A: Gen.*, **388**, 141 (2010).
- I. Agirrezabal-Telleria, J. Requies, M. B. Güemez and P. L. Arias, *Appl. Catal. B: Environ.*, **145**, 34 (2014).
- A. J. Crisci, M. H. Tucker, M.-Y. Lee, S. G. Jang, J. A. Dumesic and S. L. Scott, *ACS Catal.*, **1**, 719 (2011).
- A. S. Dias, M. Pillinger and A. A. Valente, *J. Catal.*, **229**, 414 (2005).
- C. García-Sancho, I. Agirrezabal-Telleria, M. B. Güemez and P. Maireles-Torres, *Appl. Catal. B: Environ.*, **152-153**, 1 (2014).
- I. Agirrezabal-Telleria, A. Larreategui, J. Requies, M. B. Güemez and P. L. Arias, *Bioresour. Technol.*, **102**, 7478 (2011).
- A. S. Dias, M. Pillinger and A. A. Valente, *Appl. Catal. A: Gen.*, **285**, 126 (2005).
- A. S. Dias, S. Lima, D. Carriazo, V. Rives, M. Pillinger and A. A. Valente, *J. Catal.*, **244**, 230 (2006).
- I. Agirrezabal-Telleria, F. Hemmann, C. Jäger, P. L. Arias and E. Kemnitz, *J. Catal.*, **305**, 81 (2013).
- M. M. Antunes, S. Lima, A. Fernandes, J. Candeias, M. Pillinger, S. M. Rocha, M. F. Ribeiro and A. A. Valente, *Catal. Today*, **195**, 127 (2012).
- A. Chareonlimkun, V. Champreda, A. Shotipruk and N. Laosiripojana, *Fuel*, **89**, 2873 (2010).
- I. Sádaba, S. Lima, A. A. Valente and M. López Granados, *Carbohydr. Res.*, **346**, 2785 (2011).
- T. Suzuki, T. Yokoi, R. Otomo, J. N. Kondo and T. Tatsumi, *Appl. Catal. A: Gen.*, **408**, 117 (2011).
- S. J. You, Y. T. Kim and E. D. Park, *React. Kinet. Mech. Catal.*, **111**, 521 (2014).
- K. Tanabe and W. F. Hölderich, *Appl. Catal. A: Gen.*, **181**, 399 (1999).
- W. Hongsiri, B. Danon and W. d. Jong, *Ind. Eng. Chem. Res.*, **53**, 5455 (2014).
- L. R. Ferreira, S. Lima, P. Neves, M. M. Antunes, S. M. Rocha, M. Pillinger, I. Portugal and A. A. Valente, *Chem. Eng. J.*, **215-216**, 772 (2013).
- R. O'Neill, M. N. Ahmad, L. Vanoye and F. Aiouache, *Ind. Eng. Chem. Res.*, **48**, 4300 (2009).
- S. J. You, N. Park, E. D. Park and M.-J. Park, *J. Ind. Eng. Chem.*, **21**, 350 (2015).
- V. Choudhary, S. I. Sandler and D. G. Vlachos, *ACS Catal.*, **2**, 2022 (2012).
- V. Choudhary, A. B. Pinar, S. I. Sandler, D. G. Vlachos and R. F. Lobo, *ACS Catal.*, **1**, 1724 (2011).
- G. Marcotullio and W. De Jong, *Green Chem.*, **12**, 1739 (2010).
- F. Salak Asghari and H. Yoshida, *Ind. Eng. Chem. Res.*, **45**, 2163 (2006).
- R. Weingarten, G. A. Tompsett, W. C. Conner Jr. and G. W. Huber, *J. Catal.*, **279**, 174 (2011).
- S. J. Dee and A. T. Bell, *ChemSusChem*, **4**, 1166 (2011).
- R.-J. van Putten, J. C. van der Waal, E. de Jong, C. B. Rasrendra, H. J. Heeres and J. G. de Vries, *Chem. Rev.*, **113**, 1499 (2013).
- B. Danon, L. van der Aa and W. de Jong, *Carbohydr. Res.*, **375**, 145 (2013).
- K. Lamminpää, J. Ahola and J. Tanskanen, *RSC Adv.*, **4**, 60243 (2014).
- S. Kim, M. Lee, E. Park, S. Lee, H. Lee, K. Park and M.-J. Park, *React. Kinet. Mech. Catal.*, **103**, 267 (2011).
- D. L. Williams and A. P. Dunlop, *Ind. Eng. Chem.*, **40**, 239 (1948).
- I. C. Rose, N. Epstein and A. P. Watkinson, *Ind. Eng. Chem. Res.*, **39**, 843 (2000).